Metals and Materials International (2022) 28:145–154
https://doi.org/10.1007/s12540-021-01036-0

Influence of Nanoparticles Reinforcements on Aluminium 6061 Alloys Fabricated via Novel Ultrasonic Aided Rheo-Squeeze Casting Method

T. Arunkumar[1] · Velmurugan Pavanan[2] · Vijay Anand Murugesan[3] · V. Mohanavel[4] · Karthikeyan Ramachandran[5]

Received: 2 March 2021 / Accepted: 28 April 2021 / Published online: 29 May 2021

Abstract
This study emphasis on a novel fabrication technique to fabricate hybrid cermets using Al 6061 alloy with nano sized SiC, Al_2O_3 and TiO_2 as reinforcements. During the fabrication process, the melted pool was ultrasonicated to disperse nanoparticles at 20 kHz for 5 min and pressure of 50 MPa was applied to eliminate voids. The influence of nanoparticles on physical, thermal and mechanical properties were evaluated by tensile, wear and thermal studies. Cermets with Al_2O_3 reinforcements showed higher mechanical performance compared to Al alloy. This enhancement could be related to the uniform distribution of Al_2O_3 with refinement in grain size of Al alloy which was observed via surface analysis. The morphological studies provided justifiable evidence of homogeneous distribution, nominal cluster along with agglomeration and cavities shrinking on the cermets. The agglomeration of nanoparticles along with SiC protected the cermet in corrosion and abrasive wear by ~ 97% and ~ 71%. The study evidenced the novel fabrication method using ultrasonic rheo-squeeze casting led to improvement in mechanical and thermal properties of the hybrid cermets.

Keywords Al 6061 Alloy · Hybrid cermets · Rheo-squeeze casting · Thermal behaviour · Tensile Behaviour · Corrosion

1 Introduction

Aluminium based alloys and composites are widely used in aerospace, automobile, marine, defence applications owing to their strength-to-weight ratio, good creep and chemical resistance along with rapid and low-cost manufacturing processes [1]. However, higher coefficient of thermal expansion (CTE), poor hardness and wear performance limit their load bearing and abrasion applications. Hence, there is a constant necessity to reinforce the Al matrix with suitable ceramic such as SiC, Al_2O_3, TiO_2 and B_4C to improve its properties [2–5]. Although in many applications the use of micro sized reinforcements has failed to provide the required strength. So, researchers have tended towards nanoparticles which need special reinforcing mechanisms such as Orowan mechanism, thermal discrepancy and load transfer mechanisms to strengthen the cermet according to applicational requirements [6–8]. Many researchers have worked on the reinforcement of aluminium alloys using single reinforcements such as SiC and TiO_2 [9, 10]. Bobic et al. reported that at high temperatures the reaction between SiC and aluminium alloys led to the formation of aluminium carbide which has resulted in increased mechanical properties of cermet but failed towards the corrosion resistance [11]. Likewise, the TiO_2 nanoparticles have proven to increase the base alloy wear resistance and density but severely reduce the thermal expansion [12]. Various reports state that single reinforcement is not sufficient to enhance all the properties of the aluminium alloys. Hence, a hybrid composite may act as a suitable alternative approach for enhancing the various characteristics of the alloys. Various researchers have studied the effect of introducing additional reinforcements towards

✉ Karthikeyan Ramachandran
K1825123@kingston.ac.uk

T. Arunkumar
arunmailinbox@gmail.com

1 Department of Mechanical Engineering, CMR Institute of Technology, Bengaluru, India

2 School of Mechanical Engineering, Shri Ram Murti Smarak College of Engineering and Technology, Bareilly, UP, India

3 Department of Mechanical Engineering, Kongu Engineering College, Erode, India

4 Department of Mechanical Engineering, Bharath Institute of Higher Education and Research, Chennai, India

5 Department of Aerospace and Aircraft Engineering, Kingston University, Roehampton Vale Campus, London SW15 3DW, UK

the aluminium alloys and successfully achieved improved properties. Kannan et al. compared the composite Al7075/SiC with and without Al_2O_3 reinforcement fabricated by stir casting where he justified that the UTS and hardness of the cermet enhanced by 60.1% and 80% relative to base alloy and 17.4% and 13.7% in SiC reinforced cermets [13]. Likewise, Altinkok et al. reported that the wear resistance of hybrid cermet (SiC/Al_2O_3) was significantly increased from single composite due to fine particle and interfacial bonding strength of alumina which hardened the cermet [14]. Studies revealed that the increase in hardness and other mechanical properties of the cermets could be due to hard reinforcements and other reinforcing mechanisms which act as the major reason by accumulating the reinforcing particles into molten alloys along with increasing dislocation density of the cermets [15].

Although, the overall properties of hybrid cermets also depend on the fabrication techniques associated with the alloys [16–18]. Various fabrication techniques such as infiltration or casting process is being employed for the production of hybrid cermets. However, casting techniques are being preferred over infiltration due to the lower cost, rapid structure formation and simpler mass production. Casting techniques such as stir casting, compo casting, squeeze casting and other modern techniques such as Rheo or vacuum die castings are more common techniques involving molten metal as medium [19, 20]. However, the incorporation of oxide powders into molten metals lead to non-homogenous distribution, accumulation and cluster formation of the powders onto the surfaces [21]. To circumvent this common problem associated with stir casting techniques many researchers came up with different techniques such as impellers, stirrers and ultrasonication techniques prior to fabrication. Techniques like Rheo-casting were brought into place of stir casting to reduce the cavitation on alloys which was further enhanced by ultrasonication process [22]. Shamsipour et al. studied the fractures on the different casting technique fabricated Al/Al_2O_3 based cermets with help of magnetic stirrer and determined that compo casting led to reduced dimples with more uniform distribution than sand casting [23]. However, electromagnetic stirrers were further utilised to overcome the problems associated with magnetic stirrers as the economical aspect of mass production was affected. To circumvent this problem, Shamsipour et al. utilized electromagnetic stirrers to fabricate aluminium matrix nanocomposites by optimising the parameters which led to superior wear behaviour [24]. Further, study showed the intermetallic particles were evenly dispersed with lower stress concentration points throughout the Al-Si metal matrix when using electromagnetic stirrers [25]. Even with these techniques, there have been few reports that state that ultrasonic assisted double casting techniques could hardly eliminate the porosity due to lack of external pressure. Hence, Hajjari et al. induced external pressure while fabricating hybrid Al alloys using squeeze casting and proved that the surfaces have clear microstructural refinement with reduced porosity. However, the distribution of the particles was not homogenous enough through the surfaces [26].

After a detailed literature study, various researchers have estimated the mechanical, tribological properties by single or multiple reinforcements with aluminium alloy along with the need for the aiding tool for proper distribution of powders into the molten metals. However, until today the research gaps on the aluminium 6061 alloys with reinforcements of SiC/TiO_2 combinations are limited with no exploration into the different properties while combining fabrication techniques of rheo, ultrasonication and squeeze casting process. Hence this works intends to fulfil the research gap by studying the effects of nanoparticle reinforcements ($SiC/Al_2O_3/TiO_2$) on the physical, thermal and mechanical properties of aluminium 6061 alloys fabricated via a novel ultrasonic aided rheo-squeeze casting method.

2 Materials and Methods

2.1 Materials

Aluminium 6061 ingot, magnesium and degasser Hexachloroethane procured from Chemco Engineering Pvt Ltd, Chennai were used for base material fabrication. Commercial Titanium Oxide (TiO_2), Silicon Carbide (SiC) and Alumina (Al_2O_3) nano powders of particle size ranging from 30-40 nm procured from MK industries, Canada were used as reinforcement for this work. Al 6061 based cermets were fabricated from a tailor-made aluminium squeeze casting machine, VB ceramics Pvt Ltd, Chennai.

2.2 Fabrication Process

Table 1 illustrates the various compositions of hybrid cermets of Aluminium 6061 with various nanoparticle reinforcements which were fabricated through novel process methods as shown in the flowchart (Fig. 1). Initially, various combinations of nanoparticles (2% SiC + 3% Al_2O_3 and 2% SiC + 3% TiO_2) were uniformly blended using a ball mill (SPEX 8000D, Ukraine) at a speed of 300 rpm for 1

Table 1 Composition of Samples and its notations

Sample notations	Composition
AL	Aluminium 6061
ALS	Aluminium 6061 + 2% SiC
ALSA	Aluminium 6061 + 2% SiC + 3% Al_2O_3
ALST	Aluminium 6061 + 2% SiC + 3% TiO_2

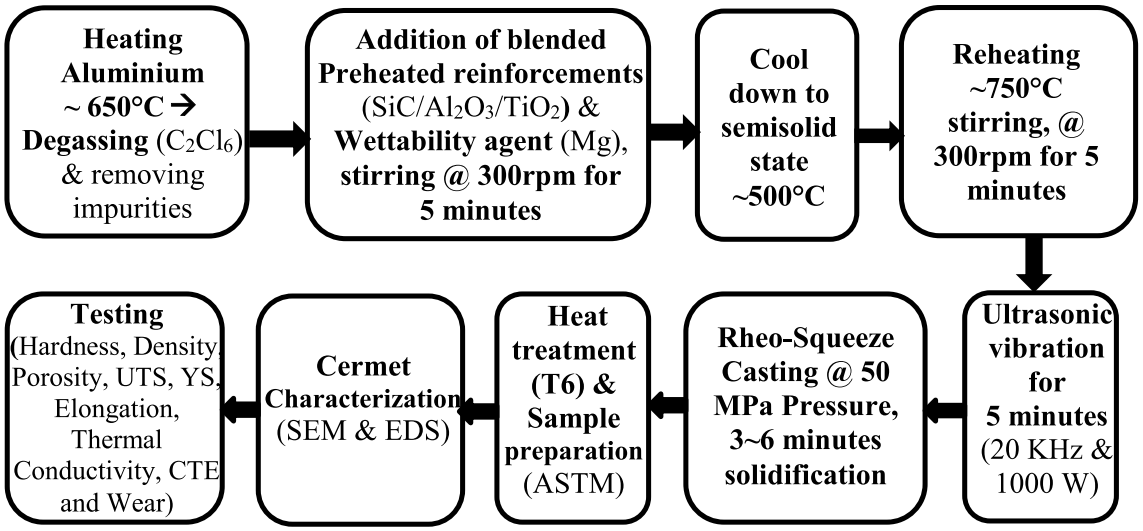

Fig.1 Flowchart of novel process for fabrication and evaluation of hybrid cermets

h. Further, the base alloy (Al 6061) ingot was heated to 650 °C in a stir casting machine and C_2Cl_6 was added into the molten alloy liquid for degassing the alloy. Subsequently, the preheated (300 °C) and ball milled nanoparticle mixtures and wetting agent (Mg) were added into the molten liquid with constant stirring speed of 300 rpm for 5 min using a mechanical impeller. The addition of degassing agents and preheating of the reinforcement will remove the excess gases around the molten alloy which reduce the oxidation. The molten liquid was cooled down into a semisolid state around 500 °C which could eventually break down the clusters/agglomeration of reinforcements at low temperature viscosity. The semi-solid molten liquid was reheated above its melting point at a temperature of 750 °C with constant stirring speed of 300 rpm for 5 min to reduce the cluster formation and further improve the wettability. This process could allow the nanoparticles to penetrate into the molten metal by breaking agglomerations leading to improved homogeneous distribution [27]. For even better distribution, an ultrasonic probe was inserted into the molten liquid and a high frequency sonication was carried out at 20 kHz for 5 min to disperse the nanoparticles homogeneously. The acoustic waves streams of the sonicator burst the bubbles formed due to transitional pressure and temperature variations and disperse the nanoparticle reinforcements eventually. Further, the molten liquid was poured into a preheated (400 °C) steel die and squeezed at a pressure of 50 MPa with 3–6 min of solidification time and cooled down to room temperature. The intention of preheating the die steel is to avoid the local stress concentration. Finally, the solidified cermet bars were released from steel die and heat treated as per T6 procedure i.e., 530 °C for 5 h followed by cold water quenching and aging at 160 °C for 24 h.

2.3 Sample Preparation, Characterisation, and Testing

The heat-treated cermets (150 × 150 × 50 mm) were machined as per ASTM standards for various testing. The surface topographies of the samples and oxide nano-powders were obtained using SEM (ZEISS SUPRA 55). Simultaneously quantitative elemental analysis was conducted on the cermets. The density of the cermets were measured by Archimedes method of liquid displacement with water as liquid medium and porosity (%) was calculated from density. The hardness test was conducted using Vickers hardness machine (Krystal Elmec, India) with diamond indenter at 10 N load and 20 s dwell time as per ASTM E92. The average grain size of the samples was calculated by the line intercept method (ASTM E112—13) from microstructure images with the help of ImageJ software. Tensile tests were conducted (UTM Zwick, Germany) as per ASTM E8/E8M-11 standard with displacement of 0.5 mm/minute. The wear behaviour of the cermets were also studied using pin on disk method (DUCOM TR-20LE-PHM-400) as per ASTM G99 standards. The wear test conditions were room temperature with ambient humidity and varying load (20 to 50 N) with sliding speed and distance of 2 m/s and 1200 m. The CTE (Coefficient of thermal expansion) was measured under argon atmosphere and thermal conductivity was measured according to ASTM E1225-13. The corrosion polarisation of the cermets were conducted with Ag/AgCl as reference electrode and Pt as counter electrode with 3.5% NaCl electrolyte [28].

3 Results and Discussion

3.1 Novelty of Fabrication Technique

Figure 1 shows the flow chart of the novel technique utilized for the fabrication of the hybrid cermets. As shown in Fig. 1, the fabrication process has been split into different steps as explained in the previous section. The base alloy was melted at a temperature of 650 °C and oxide nanoparticles are added in a preheated condition of 300 °C to reduce the oxidation using a mechanical impeller with continuous stirring at speed of 300 rpm for 5 min to avoid cluster formation owing to high viscosity at lower temperatures and liquid is cooled to a semi-solid state [29]. Further reheating was undertaken above the melting point of base alloy at a temperature of 750 °C to enhance the distribution of oxide particles. Acoustics aides ultrasonication were performed at high frequency of 20 kHz for 5 min to increase the homogeneous distribution of the nanoparticles which also resulted in reduced cavitation and porosity [30]. The acoustics waves formed through the ultrasonication process further breaks the clusters of nano-oxide particles which spread the particles homogeneously throughout the molten pool. Further double squeeze casting was carried out with an external pressure to further reduce porosities. Even though squeeze casting was successful in providing a high-density alloy, the external pressure provided the sample with clear surfaces along with fine microstructural refinement with relatively low porosity [26].

3.2 Morphology and Elemental Analysis

Scanning electron microscopic images of the nano-powders were obtained and morphologies of the powders were studied. The SEM Figures were taken at a constant scale of 200 nm to understand the morphology. The Fig. 2(a) shows the morphology of SiC ceramic. The α-SiC was hexagonal in shape with particle size of > 40 nm [31]. However, the TiO_2 and Alumina presented a rutile and tetragonal structure with a particle size range of ~ 40–50 nm as shown in Fig. 2(b & c). Figure 3 illustrates the morphology of the Al 6061 alloy along with different reinforcement combinations of ceramics nanoparticles. Figure 3(a) shows the presence of open pores throughout the Al alloy and Fig. 3(b, c & d) shows the presence of various nanoparticles incorporated into the Al alloy which are visible under higher magnification. The presence of pores in the Al alloy in Fig. 3(a) evidence that the squeeze casting of the Al alloys even with an external pressure presented with pores throughout the surfaces. This could have been due to cavitation on the molten metal while utilizing a mechanical impeller which led to higher viscosity at lower temperature at cooling down [32]. Figure 3 (b, c & d) evidences the distribution of nanoparticles along with nominal agglomeration and clusters with reduced porosity

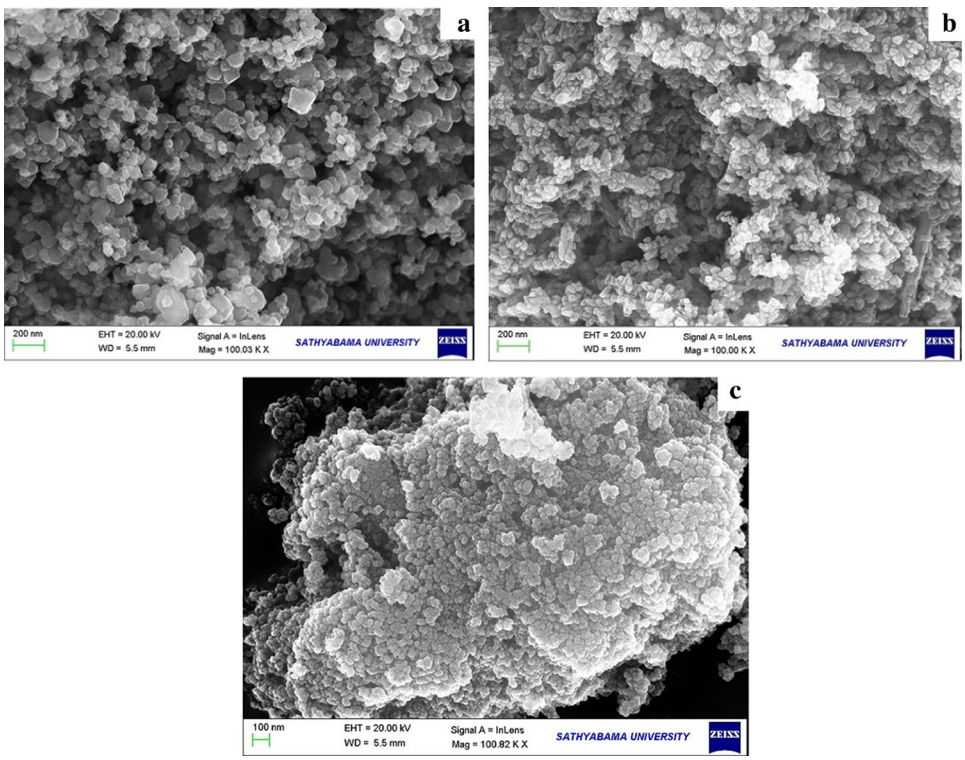

Fig.2 Scanning electron images of nanoparticles **a** SiC **b** TiO_2 **c** Alumina

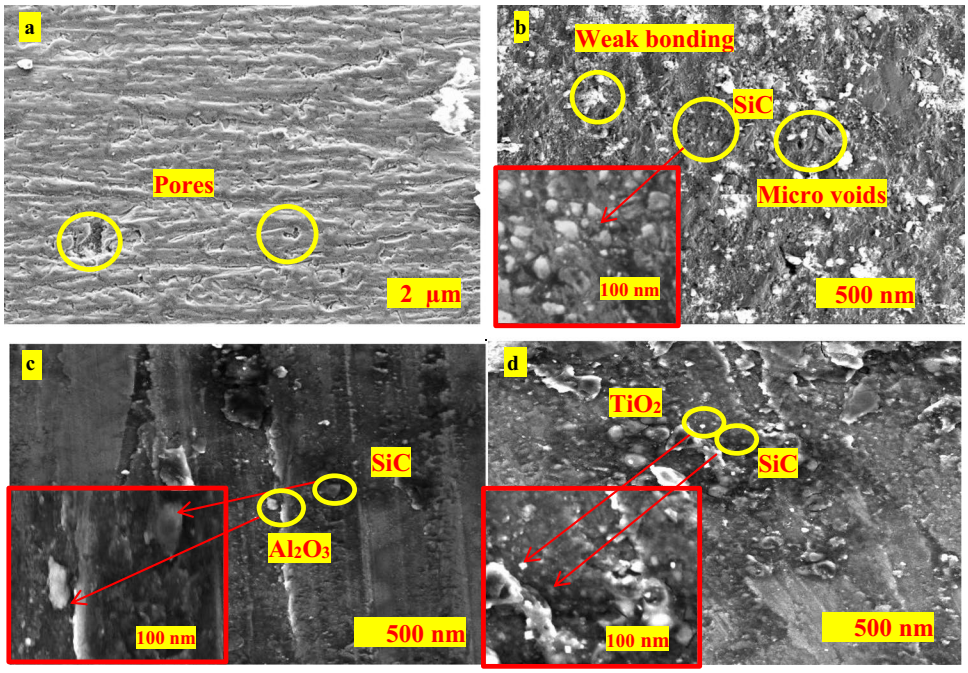

Fig. 3 Morphology of samples **a** AL, **b** ALS, **c** ALSA, and **d** ALST

in the cermets fabricated through ultrasonic assisted rheo-squeeze casting method. The increased distribution may have been due to the mechanical stirring using an impeller at a temperature of 650℃ which led to enhanced particle distribution and a decrease in agglomeration size as a result of higher friction. Also, ultrasonication at a higher temperature in lower viscosity increases the maximum distribution of nanoparticles. The ultrasonic waves were responsible for the breakdown of clusters of nanoparticles followed by homogenous distribution in the molten liquid. Even though the homogenous distribution was not perfect as there were small clusters of nano-powders throughout the surfaces as reported by Shabini et al. with B_4C particulates [33]. On the other hand, the average grain size of the hybrid cermets has been drastically refined up to 52% from the aluminium base alloy. Figure 4 shows the quantitative analysis of the cermets which proves the presence of Aluminium along with SiC, TiO_2, Al_2O_3 and Mg. The wetting agent magnesium peaks were observed in the entire spectrum showing that Mg was properly incorporated and binds the reinforcement particles. The presence of carbon and oxygen in Fig. 4(a to d) proves the oxidation of materials even at lower temperatures. In Al-SiC composites, the reaction between Al and SiC could form an undesired composite of Al_4C_3 which could have a concerning effect in the corrosion resistance of the material which is evidenced by the presence of Al and C in the elemental analysis [34]. The smooth surface of the cermets proves the fine-grain reinforcement achieved by the fabrication technique along with no reactions on the surfaces. The composite shows a strong metallurgical bonding between the Al and other particles with reduced porosity owing to the pressure of 50 MPa applied towards the fabrication technique.

3.3 Densification, Porosity and Hardness

Figure 5 and Fig. 6 illustrate the Vickers hardness, density, porosity and grain size of the samples. The composites exhibited higher densities than Al alloy with an increase of 6.3%, 7.57%, and 7.53%. The accumulation of reinforcements into molten alloys as well as the dislocation density in the whole cermet is increased due to the huge difference in the thermal expansion between metal and ceramics. It has been found that with an increase in the nanoparticle content, an increase in density has been noted. This increase may have been due to the addition of ceramic particulates which have been reported by many researchers [35, 36]. Likewise, the hardness values were increased from 0.925 GPa (Table 2) for the base alloy to 1.035 GPa (11.89% increased) for the accumulation of 2% SiC (ALS). Similarly, 2% SiC + 3% Al_2O_3 (ALSA) and 2% SiC + 3% TiO_2 (ALST) samples hardness were also increased by 1.1 GPa (18.91%) and 1.128 GPa (21.94%) as compared to base alloy. The ALST sample had the highest hardness than other samples because of the high dense TiO_2 which helps in directly strengthening the matrix, thus preventing dislocation and grain growth. The increase in the hardness values has been reported by many researchers with varied reasoning such as particle refinement, volume fraction and use of hard ceramics. Roy and Hoskins et al. reported that the reinforcing Al alloy with SiC, Alumina and aluminide particulates would result in higher hardness [36, 37].

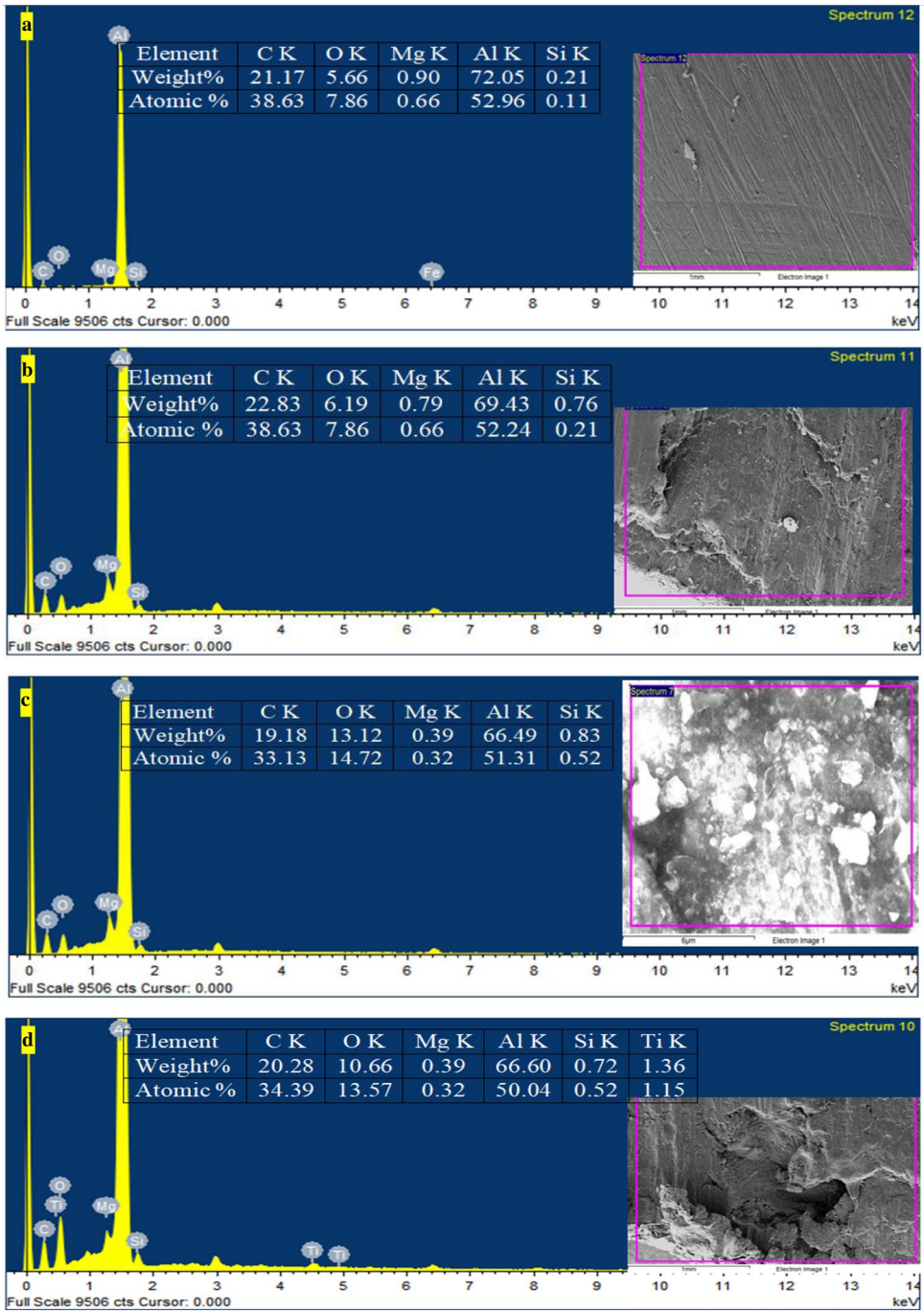

Fig. 4 Elemental analysis of samples **a** AL, **b** ALS, **c** ALSA, and **d** ALST

Likewise, Lloyds and Hutchings stated that the addition of hard ceramics could increase the hardness in Al-based metal matrix composites [35, 39]. But in this case, the increase in hardness could have been the result of uniform dispersal of the nanoparticles in the composites owing to the ultrasonication along with good interfacing bonding and structure of the MMCs obtained by squeeze pressure of 50 MPa applied onto the composites [40]. Furthermore, with an increase in the nano-sized particulate reinforcements in the metal matrix composites, the porosity of the cermets decreased by 83.38% (ALS), 86.85% (ALSA) and 84.59% (ALST). This drastic decrease in the porosity could have been contrary to other research on Al metal matrix composites [36]. The reduction in the porosity could be attributed to the novel fabrication technique which involved squeeze casting and ultrasonication which uniformly distributed the particles throughout the surfaces. It can also be noted that there has been a slight increase in porosity in ALST compared to ALS and ALSA, this could have been due to the addition of TiO_2 which could

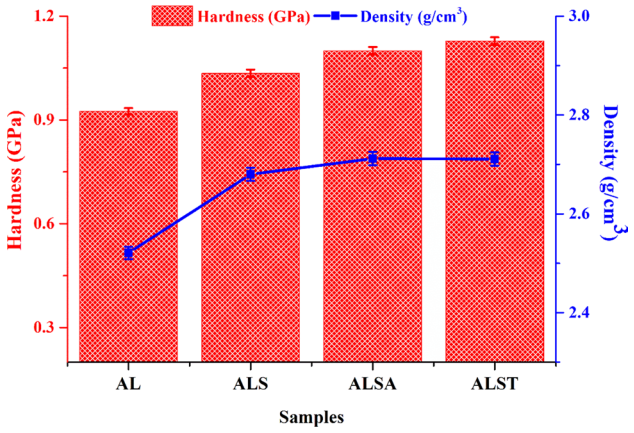

Fig. 5 Vickers hardness and density of fabricated hybrid cermets and Al 6061 alloy

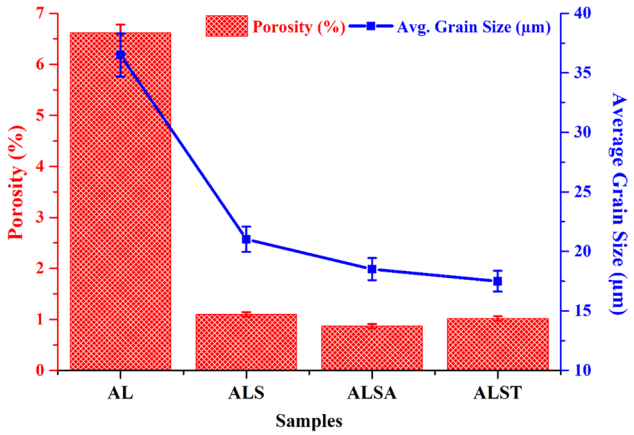

Fig. 6 Average grain size and porosity (%) of fabricated Al 6061 alloy and hybrid cermets

have been due to poor interfacing bonding between the TiO_2 and SiC particles [41]. Overall, the effect of squeezing pressure, nano-particle dispersal, reinforcement strong bonding and better refinement is evidenced by increased hardness and density.

3.4 Tensile Behaviour

The UTS and YS of the cermet materials are increased with a decrease in elongation as shown in Fig. 7. The UTS and YS of ALS cermet increased by 10.39% and 3.9% whereas elongation dropped down by 7.15% compared to the base alloy. Likewise, the ALSA composite also showed an increase of 16.87% and 8.4% in UTS and YS. The tensile strength of the composites along with Al alloy is high compared with other literatures [26, 42]. This increase in tensile strength could have been due to the novel fabrication technique which provided high interfacial bonding along with better grain refinement. The increase in the tensile strength of the ALS is stated to be attributed to two different mechanisms i.e., grain refinement and addition of SiC nanoparticles which have higher tensile strength compared with Al [42, 43]. Also, the Al-SiC chemical enhanced the interfacing bonding between the matrix and reinforcement which led to increased strength [44]. Further, the reinforcement of Al alloy with SiC and Alumina in ALSA led to increased tensile and yield strength compared to all other hybrid composites and Al base alloy. The presence of hard reinforcements of SiC and Al_2O_3 on the softer Al matrix leads to an increase in dislocation density due to thermal mismatch between Al and ceramics. This dislocation energy increase contributes towards the increase in the ultimate tensile strength which is observed in the literature [45]. But the steep drop in UTS of ALTS composite could be attributed to the presence of TiO_2 nanoparticles which have a higher CTE compared to Alumina and SiC. This CTE of TiO_2 could have been the reason for a reduction in the tensile strength due to the dislocation densities along with higher elastic moduli mismatch which could result in a reduction of tensile strength but not in hardness. The hybrid composites with oxide-based nanoparticles show an increased tensile strength with a constant loss in strain. The decrease in elongation could be due to the addition of hard and brittle natured ceramics which increase the embrittling effect in the Al base matrix. The constant escalation in hybrid composites over the Al base alloy is generally due to the overall grain reduction, homogeneous distribution and interfacing bonding between the matrix and ceramic reinforcement.

Table 2 Properties of fabricated Al 6061 alloy and hybrid cermets

Samples	Density (g/cm^3)	Hardness GPa	Avg.Grain size (µm)	Porosity %	UTS MPa	YS MPa	E %	TC W/m.K	CTE X10^{-6} / ^{O}C
AL	2.521	0.925	36.50	6.62	270.2	258.12	11.2	162	22.8
ALS	2.680	1.035	21.03	1.10	298.3	268.20	10.4	156	20.7
ALSA	2.712	1.100	18.52	0.87	315.8	279.81	9.5	141	18.3
ALST	2.711	1.128	17.50	1.02	305.8	273.28	9.8	132	18.2

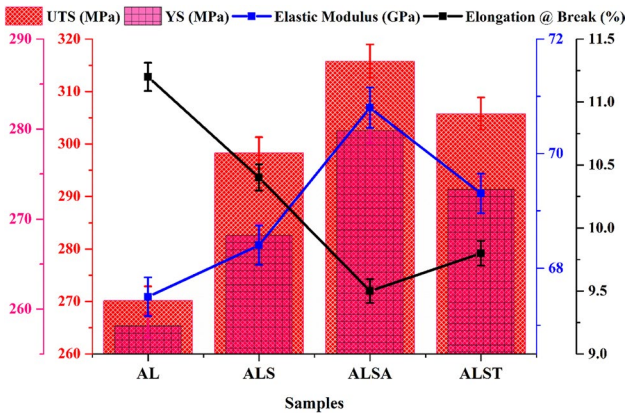

Fig. 7 UTS, Yield strength, elastic modulus and elongation of the samples

3.5 Thermal Conductivity and Thermal Expansion

Figure 8 illustrates the variation in thermal conductivity (TC) and thermal expansion coefficient (CTE) with reinforcement of nanoparticles into the base material. The ASL showed a reduction in TC and CTE value by 3.7% and 9.21% relative to Al 6061 whereas the ALSA and ALST showed a reduction of 12.96% and 19.73% in TC and 18.51% and 20.17% in CTE compared to Al 6061. The reduction in the TC and CTE of the material could have been due to CTE mismatch between the ceramic reinforcement and Al alloys. The addition of nano-ceramic particles could reduce the thermal expansion and other CTE based on the rule of mixtures as the CTE of ceramics is lower than the Al alloys. Whereas CTE mismatch cannot be the only factor to blame for reduction, Huber et al. revealed that the CTE also depends on the matrix alloy and architecture of reinforcement along with plasticity of matrix [46]. Many authors have studied the thermal expansion of metal matrix composites by formulating different mathematical models but none of the models predicted the microstructural change distortion in the lattice parameters including grain size. The reduction in TC and CTE of the hybrid composites could have been due to the lattice distortion at the mechanical and physical interfaces of matrix and reinforcements. These lattice distortions would lead to reduced particle size with the induction of thermal stress which could act on the interface resulting in reduced CTE.

3.6 Wear Behaviour

Specific wear rate (SWR) of the cermet materials is varying with the effect of increased load and accumulation of nanoparticles under constant speed as shown in Fig. 9. The wear rate at a load of 20 N of ALS, ALSA and ALST cermets were significantly reduced by 39.74%, 55.63% and 71.52% respectively to the base material. Likewise, for cermet ALS, ALSA and ALST value of SWR concerning load (30,40 & 50 N) were significantly reduced in the same trend relative to the base material. It is noted that the specific wear rate of the composites is lesser than that of Al alloys irrespective of the load or sliding speed with an increase in specific wear rate is noted with an increase in applied load. In both Al alloys and composites under dry conditions, the loss in volume corresponded towards the increase in load. The abrasion rate in both cases contributed towards the material separation from the surfaces followed by maximum material loss. However, the SWR of the cermets was lower than the base material due to the presence of high wear resistance ceramics as reinforcements to the matrix of Al which prevented the deformation and loss of volume. While observing the Al alloys under dry conditions, it can be stated that the material operates

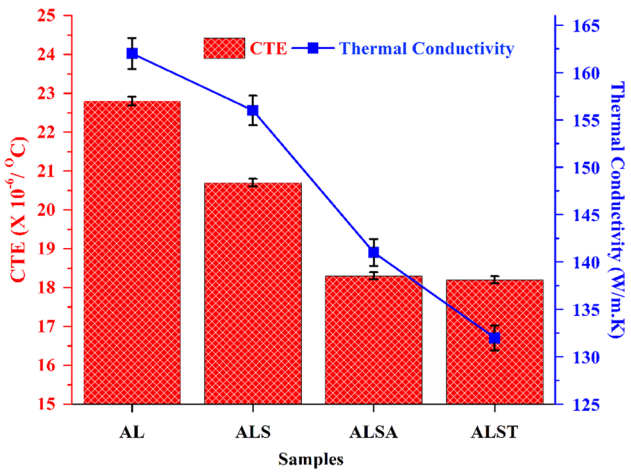

Fig. 8 CTE and thermal conductivity of the samples

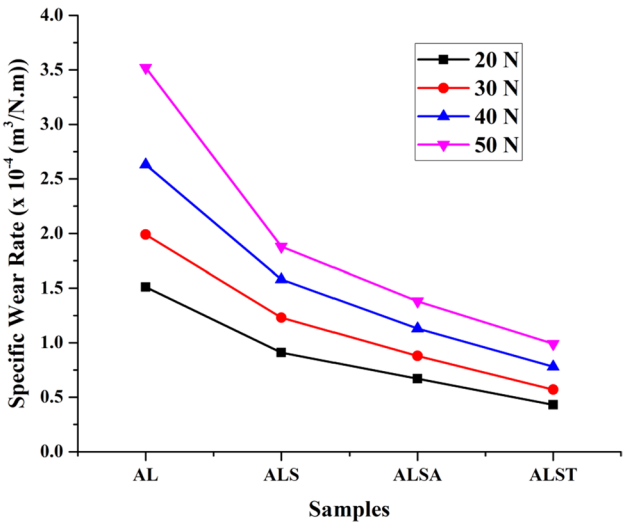

Fig. 9 Specific wear rate of the samples against various loads

under a severe regime of wear with severe plastic deformation which is irrespective of contact stress. These results are consistent with researchers [47, 48]. However in composite samples, the specific wear rate decreased with increasing load, this decrease could have been due to the temperature-induced between the abrasive disk material and sample results in softening of the matrix which affects the bonding strength of ceramics and Al matrix which significantly result in breakage of small ceramic particles. Similar observations were observed by researchers where the wear resistance of softer material was lesser due to rapid abrasion between disc and specimen [49, 50]. Two different mechanisms namely deformation and adhesion were observed from the worn surfaces from the composites. Delamination was observed on the samples of the AL and ALS samples where severe wear was recorded and adhesion according to Archard's law was observed in other hybrid cermets where the ceramics were able to hold down the wear by forming oxide layers namely metal matrix layers (MML) which had a better impact on the tribological characteristics of the composites [51].

3.7 In-situ Corrosion

Table 3 plots the calculated experimental values of the corrosion potential (E_{corr}), corrosion current density (I_{corr}) and corrosion rate obtained from the Tafel plot represented in Fig. 10. Corrosion parameters from the Tafel plots were calculated based on the potential values of the cathodic and anodic regions from the Tafel plot. The ALS cermet value of E_{corr} and I_{corr} were decreased by 15.37% and 67.5% while the rate of corrosion has decreased or protected by 68.59% as compared to the base material. Likewise, ALSA, ALST samples rate of corrosion has decreased or protected significantly by 96.69% and 97.90% as compared to the base alloy. The current density extrapolated values of corrosion rate and potential of Al alloys and hybrid composites which represents a shift towards higher current densities. The positive shift in E_{corr} and decrease in I_{corr} confirms that the corrosion rate decreases along with the addition of nanoparticles into the alloys. The decrease in I_{corr} also confirms that the anodic current of the corrosion reduced could be due to the uniform distribution of nanoparticles which offers greater resistance.

Table 3 In-situ corrosion rate of Al 6061 alloy and hybrid cermets

Samples	I_{corr} (μA cm^{-2})	E_{corr} (mV)	Rate of Corrosion (μm/year)	Protected efficiency %
AL	4.40	−710.46	47.73	–
ALS	1.43	−601.22	14.99	68.59
ALSA	0.15	−558.6	1.58	96.69
ALST	0.10	−530.7	1.00	97.90

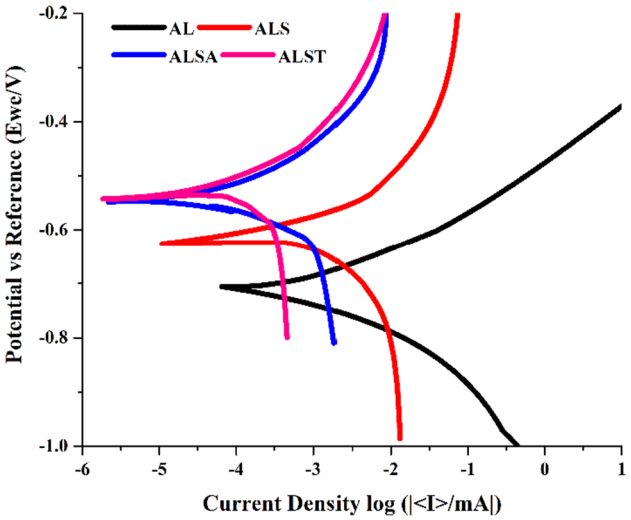

Fig. 10 Tafel Plots of the samples

The positive shift verified on the E_{corr} value leads to the conclusion there is a simultaneous decrease of corrosion rate in the composites which was observed by Abdel et al. or the Zn and Ni materials [52]. It is revealed that the accumulation of nanoparticle reinforcements with uniform distribution in the entire cermet can be protecting in-situ corrosion for a long period.

4 Conclusion

Al 6061 alloy reinforced with various combinations of nanoparticles were prepared through novel ultrasonic aided rheo-squeeze casting route. The novel method provided a high-density hybrid cermets with lower porosity and high grain refinement with nominal level of agglomeration of nanoparticles. Mechanical properties viz., hardness, tensile strength and wear behaviour of the cermets have been investigated and the results showed that the hybrid cermets showed increased mechanical properties along with higher corrosion resistance with increasing ceramic particles in Al alloy. The results of ultimate tensile strength of ALS, ALSA and ALST increased by 21.36%, 35.68% and 27.5% compared with the base alloy of Al 6061. Likewise, the hardness also increased by 10.29%, 14.28% & 15.7% with the base materials. The wear and corrosion rate of the hybrid cermets also reduced drastically by 71.52% (20 N load) and 97% for ALST composite than the Al 6061 alloy. The formation of Aluminium Carbide in ALSA and ALST cermets increased the corrosion rate compared with ALS and base material. Overall, the novel fabrication technique led to an increase in mechanical, tribological and corrosion nature of the Al hybrid cermets which can be further influenced

in automotive and aerospace sectors owing to improved mechanical properties compared to Al alloys.

Acknowledgements Corresponding author Karthikeyan Ramachandran would like to acknowledge the support provided by Kingston University, London by providing him with studentship for his PhD research.

References

1. F. Khodabakhshi, A.P. Gerlich, P. Svec, Mater. Sci. Eng. A **698**, 313 (2017)
2. Yashpal, Sumankant, C.S. Jawalkar, A.S. Verma, N.M. Suri, Mater. Today **4**, 2927 (2017)
3. B.T.S. Al-Mosawi, D. Wexler, A. Calka, Characterization and properties of aluminium reinforced milled carbon fibres composites synthesized by uniball milling and uniaxial hot pressing. Met. Mater. Int. (2020). https://doi.org/10.1007/s12540-020-00644-6
4. X. Bin, W. Xiaogang, H. Xiaohu, Y. Dawei, Rare Metal Mat. Eng. **43**, 2089 (2014)
5. B. Gobalakrishnan, C. Rajaravi, G. Udhayakumar, P.R. Lakshminarayanan, Effect of ceramic particulate addition on aluminium based ex-situ and in-situ formed metal matrix composites. Met. Mater. Int. (2020). https://doi.org/10.1007/s12540-020-00868-6
6. P.S.S. Ratna Kumar, D.S. Robinson Smart, S. John Alexis, J. Asian Ceram. Soc. **5**, 71 (2017)
7. T. Arunkumar, G. Anand, R. Subbiah, R. Karthikeyan, J. Jeevahan, Effect of multiwalled carbon nanotubes on improvement of fracture toughness of spark-plasma-sintered yttria-stabilized zirconia nanocomposites. J. Mater. Eng. Perform. (2021). https://doi.org/10.1007/s11665-021-05562-1
8. T. Arunkumar, R. Karthikeyan, R. Ram Subramani, K. Viswanathan, M. Anish, Int. J. Ambient Energy **41**, 452 (2020)
9. M.O. Shabani, F. Heydari, Prot. Met. Phys. Chem. **55**, 748 (2019)
10. S.M. Almotairy, A.F. Boostani, M. Hassani, D. Wei, Z.Y. Jiang, Met. Mater. Int. **27**, 851 (2021)
11. B. Bobić, S. Mitrović, M. Babić, I. Bobić, Tribol. Ind. **32**, 3 (2010)
12. M. Gupta, M.O. Lai, C.Y.H. Lim, J. Mater. Process. Tech. **176**, 191 (2006)
13. C. Kannan, R. Ramanujan, J Adv. Res. **8**, 309 (2017)
14. N. Altinkok, I. Ozsert, F. Findik, Acta Phys. Pol. A **124**, 11 (2013)
15. R. Casati, M. Vendani, Metals **4**, 65 (2014)
16. W.Y. Zhang, Y.H. Du, P. Zhang, J. Alloy. Compd. **787**, 206 (2019)
17. X. Chen, Z. Xu, D. Fu, H. Zhang, J. Teng, F. Jiang, Met. Mater. Int. **27**, 1880 (2021)
18. V. Gholipour, M. Shamanian, A. Ashraf, A. Maleki, Development of aluminium-nanoclay composite by using powder metallurgy and hot extrusion process. Met. Mater. Int. (2020). https://doi.org/10.1007/s12540-020-00791-w
19. A. Thirugnanasambandam, N. Joy, A. Mariadhas, K.S. Sridhar Raja, A.K. Tiwari, B.V.S. Krishna, AIP Conf. Proc. **2311**, 080016 (2020)
20. A.K. Sharma, R. Bhandari, A. Aherwar, C.P. Bretotean, Mater. Today **27**, 1608 (2020)
21. X. Kai, S. Huang, L. Wu, R. Tao, Y. Peng, Z. Mao, F. Chen, G. Li, G. Chen, Y. Zhao, J. Mater. Sci. Technol. **35**, 2107 (2019)
22. M.R. Ghomashchi, A. Vikhrov, J. Mater. Process. Tech. **101**, 1 (2000)
23. M.O. Shabani, A. Baghani, A. Khorram, F. Heydari, Silicon **12**, 2977 (2020)
24. M. Shamsipour, Z. Pahlevani, M.O. Shabani, A. Mazahery, Kovove Mater. **55**, 33 (2017)
25. M.O. Shabani, F. Heydari, A. Khorram, Silicon **11**, 2539 (2019)
26. E. Hajjari, M. Divandari, Mater. Design **29**, 1685 (2008)
27. J. Li, S. Lu, S. Wu, Q. Gao, Ultrason. Sonochem. **42**, 814 (2018)
28. T. Arunkumar, S. Ramachandran, Int. J. Ambient Energy **38**, 781 (2017)
29. A.T. Dinsdale, P.N. Quested, J. Mater. Sci. **39**, 7221 (2004)
30. P. Madhukar, N. Selvaraj, R. Gujjala, C.S.P. Rao, Ultrason. Sonochem. **58**, 104665 (2019)
31. T. Arunkumar, R. Karthikeyan, R. Ram Subramani, M. Anish, J. Theertagiri, Curr. Anal. Chem. **16**, 1 (2020)
32. A. Jahangiri, S.P.H. Marashi, M. Mohammadaliha, V. Ashofte, J. Mater. Process. Tech. **245**, 1 (2017)
33. A. Mazahery, M.O. Shabani, J. Mater. Eng. Perform. **21**, 247 (2012)
34. G.B.V. Kumar, C.S.P. Rao, N. Selvaraj, J. Min. Mater. Charc. Eng. **10**, 59 (2011)
35. D.J. Lloyd, Int. Mater. Rev. **39**, 1 (1994)
36. P.N. Bindumadhavan, T.K. Chia, M. Chandrasekaran, H.K. Wah, L.N. Lam, O. Prabhakar, Mater. Sci. Eng. A **315**, 217 (2001)
37. D. Roy, B. Basu, A.B. Mallick, Intermetallics **13**, 733 (2005)
38. F.M. Hosking, F.F. Portillo, R. Wunderlin, R. Mehrabian, J. Mater. Sci. **17**, 477 (1982)
39. I.M. Hutchings, Mat. Sci. Tech. **10**, 513 (1994)
40. R.L. Deuis, C. Subramanian, J.M. Yellup, Wear **201**, 132 (1996)
41. G. Elango, B.K. Raghunath, Procedia Engineer. **64**, 671 (2013)
42. A.I. Khdair, A. Fathy, J. Mater. Res. Technol. **9**, 478 (2020)
43. A. Mazahery, M.O. Shabani, T. Nonferr. Metal. Soc. **22**, 275 (2011)
44. S.S. Murugan, V. Jegan, M. Velmurugan, J. Inst. Eng. India Ser. D **99**, 71 (2018)
45. N. Radhika, T.V. Balaji, S. Palaniappan, J. Eng. Sci. Technol. **10**, 134 (2015)
46. T. Huber, H.P. Degischer, G. Lefranc, T. Schmitt, Compos. Sci. Technol. **66**, 2206 (2006)
47. S. Elomari, R. Boukhili, C. San Marchi, A. Mortensen, D.J. Lloyd, J. Mater. Sci. **32**, 2131 (1997)
48. M.J. Ghazali, W.M. Rainforth, H. Jones, Wear **259**, 490 (2005)
49. R.D. Manikonda, S. Kosaraju, K.A. Raj, N. Sateesh, Mater. Today **5**, 20104 (2018)
50. H. Turhan, O. Yilmaz, Z. Metallkd. **93**, 572 (2002)
51. D. Huang, R. Li, L. Huang, V. Ji, T. Zhang, Intermetallics **19**, 1385 (2011)
52. A.R. El-Sayed, H.S. Mohran, H.M. Abd El-Lateef, Metall. Mater. Trans. A **43**, 619 (2012)